electron-withdrawing field-inductive effect of one more fluorine substituent in the CF_4 adduct should destabilize the ion.

SO_2 and SO_2ClF are important solvents of low nucleophilicity. The present results for SO_2F_2, reaction 15, Table I and Figure 6, show that the SO_2F_2 bonding to t-Bu$^+$ is significantly weaker than that of CH_2Cl_2. Measurements of the Me$^+$ bonding to SO_2, SO_2ClF, and SO_2F_2 from this laboratory (methyl cation affinities)[6] show the bonding decreasing in the order SO_2, SO_2ClF, SO_2F_2. The same order may be expected also for bonding to more stable ions like t-Bu$^+$. On this basis one may expect that the bonding of t-Bu$^+$ to SO_2ClF will be similar to that for CH_2Cl_2. Assuming that this is the case one would expect that a plot of R$^+$–SO_2ClF bonding energies would be similar to the R$^+$$CH_2Cl_2$ plot on Figure 7, and this would mean that little differential specific nucleophilic solvation by SO_2ClF can be expected for ions R$^+$ which are fairly well stabilized, i.e., ions that fall in the flat region of the plot in Figure 7. This is a result that is anticipated from Arnett's[8,9] measurements of R$^+$ ion stabilities in SO_2ClF solution.

The bond dissociation energies $D(R^+-ClR)$ predicted by MINDO/3 are given in Table II. The fact that MINDO/3 was successful is predicting the $D(R^+-ClMe)$ energies (see Table I) lends credence also to the present data, for which experimental determinations were not made. The calculation shows that D-(R^+-ClR) decreases as the stability of R$^+$ increases, i.e., in the order R = Me, Et, i-Pr, t-Bu. These results can be compared with the trends already discussed above, i.e., the rapid decrease of $D(R^+-ClMe)$ in the above order (Table I) and the increase of $D(Me^+-ClR)$ in the above order (Table II). In the symmetric adducts R_2Cl^+, these two effects occur in opposition; however, the weakening of $D(R^+-ClMe)$ with an increase of R$^+$ stability is the stronger effect which leads to the net weakening of D-(R^+-ClR) predicted by the calculation.

Formation of Ionic Transition-Metal Carbonyl Cluster Fragments by Ion–Molecule Reactions. 1. The Cr(CO)$_6$ and Fe(CO)$_5$ Systems

DonnaJean Anderson Fredeen and David H. Russell*

Contribution from the Department of Chemistry, Texas A&M University, College Station, Texas 77843. Received January 7, 1985

Abstract: Fragment ions formed by dissociative ionization of Cr(CO)$_6$ and Fe(CO)$_5$ react readily with their respective neutrals to give ionic cluster fragments of the type M$_x$(CO)$_y^+$. The M$^+$ and M(CO)$_x^+$ reactant ions give rise to different ionic cluster fragments which undergo further reaction with neutral M(CO)$_y$. In this paper, we propose the reactivity of the ionic cluster fragments is related to the degree of coordination unsaturation. Plots of the relative reaction rate vs. electron deficiency can give some indication of the structure of the cluster fragments. This interpretation of the results suggests that some cluster fragments have multiple metal–metal bonds and/or carbonyl ligands acting as 4-electron donors. The present work emphasizes the ion–molecule reaction sequence and the degree of coordination saturation/unsaturation of the ionic cluster fragments.

The study of the chemical and physical properties of transition-metal clusters is a rapidly expanding research field.[1] The rapid growth in this area can be attributed to the development of new experimental techniques which permit detailed studies at the molecular level. For example, studies on the reactivities of single crystals provide more detailed information than methods which probe the average reactivities of bulk material.[2] The recent studies by several research groups on small bare metal clusters represent steps to refine even further these studies, i.e., the modeling of reactive sites at the molecular level.[3] It is hoped that such studies will provide important insight into the properties of transition-metal clusters which has been unobtainable from bulk studies. Over the past several years we have been studying the ion–molecule reaction chemistry of ionic transition-metal cluster fragments. The objectives of these studies include investigating the reactivities of metal ions with other metal-containing species,

characterizing these clusters with both spectroscopic methods and chemical reactivities, and utilizing these clusters as models for catalytic reactions, e.g., C–H and C–C bond-insertion reactions. In this report, the general ion-molecule reaction sequence for cluster formation for the Cr(CO)$_6$ and Fe(CO)$_5$ systems is presented.

Several reviews have appeared in the literature on the synthesis and characterization of small metal clusters, and throughout the development of ion cyclotron resonance (ICR) spectrometry, the chemistry of transition-metal ions has been an active research area.[4-14] In an early study with ICR, Beauchamp and Foster

(1) See, for example: (a) King, R. B. "Progress in Inorganic Chemistry"; Lippard, S. J.; Ed.; John Wiley & Sons, Inc.: New York, 1972; p. 287. (b) Muetterties, E. L. *Catal. Rev.*-Sci. *Eng.* 1981, 23, 69.

(2) Davis, S. C.; Klabunde, K. J. *Chem. Rev.* 1982, 82, 153.

(3) Hopkins, J. B.; Langridge-Smith, P. R. R.; Morse, M. D.; Smalley, R. E. *J. Chem. Phys.* 1983, 78, 1627.

(4) Burnier, R. C.; Byrd, G. D.; Freiser, B. S. *J. Am. Chem. Soc.* 1981, 103, 4360.

(5) Burnier, R. C.; Byrd, G. D.; Freiser, B. S. *J. Am. Chem. Soc.* 1982, 104, 3565.

(6) Byrd, G. D.; Freiser, B. S. *J. Am. Chem. Soc.* 1982, 104, 5944.

(7) Jacobson, D. B.; Freiser, B. S. *J. Am. Chem. Soc.* 1983, 105, 736.

(8) Freas, R. B.; Ridge, D. P. *J. Am. Chem. Soc.* 1980, 102, 7131.

(9) Allison, J.; Ridge, D. P. *J. Am. Chem. Soc.* 1978, 100, 163.

(10) Dietz, T. G.; Chatellier, D. S.; Ridge, D. P. *J. Am. Chem. Soc.* 1978, 100, 4905.

(11) Jones, R. W.; Staley, R. H. *Int. J. Mass Spectrom. Ion Phys.* 1981, 39, 35.

reported on the gas-phase ion–molecule chemistry of iron pentacarbonyl.[15] In this study, clusters as large as $Fe_4(CO)_{12}^+$ were formed by the reaction of Fe^+ and $Fe(CO)_x^+$ ($x = 1-4$) with $Fe(CO)_5$. This group has also reported on the formation of dinuclear species, e.g., $Fe_2(C_5H_5)_3^+$ and $Ni_2(C_5H_5)_3^+$, from ferrocene and nickelocene.[16,17] Ridge et al. have used transition-metal carbonyls as sources of metal ions,[18] studied the formation of dimetal clusters and ligand exchange reactions of gaseous ionic systems,[19] and very recently, reported on the formation of anionic clusters of $Fe(CO)_5$.[20] Freiser and co-workers have used laser ionization and ICR to study the gas-phase chemistry of metal ions. For example, they have reported on the formation of copper/iron mixed-metal clusters and numerous metal ions, e.g., the gas-phase reactions of Fe^+ with ketones and ethers.[21,22] Allison and co-workers are studying the chemistry of ionic metal centers with multifunctional organic molecules.[23] Similarly, Staley has investigated the chemistry of small (M_2^+) mixed-metal clusters from metal carbonyls.[24] Using ICR, these and related studies provide important insights concerning the stability of metal clusters,[20] relative ligand binding energies,[25] and thermochemical heats of formation of many transition-metal complexes.[26] Using an ion-beam apparatus, Beauchamp and Armentrout have studied the endothermic ion-molecule reactions of several metal ions with organic systems.[27] These studies provide important information on reaction energetics and energy breakdown graphs. In addition, Armentrout has used this same method to estimate the bond strength for Mn_2^+[28]

Using lasers and supersonic beams, Smalley et al. have recently reported on the formation of bare metal clusters.[29-33] These studies have provided an estimated bond length for Cr_2 as 1.68 ± 0.01 Å.[29] They have also examined supersonic beams of Cu_2[30] and Al[31] as well as the multiphoton ionization of metal carbonyls cooled in a pulsed supersonic beam.[32] Another area of study includes a photolytic process that converts microcrystals of $Fe(CO)_5$ into Fe_x clusters ($x = 1-30$).[33]

The studies that have been reported to date provide a foundation for understanding metal clusters and the role these clusters play in catalysis. In this report, we present the results of ion–molecule reaction studies which give rise to ionic clusters of first-row transition-metal carbonyls. The objectives of these studies are to develop methods for preparation of ionic metal clusters which can be utilized as models for catalytic reactions. The present work emphasizes the ion–molecule reaction sequence leading to cluster formation and the degree of coordination saturation/unsaturation,

Figure 1. Diagram of the experimental sequence for FTMS.

which can serve as a predictive model for the reactivity, of these ionic cluster fragments.

Experimental Section

All experiments were carried out with a standard Nicolet FTMS-1000 equipped with a 3T magnet and a cubic (2.5 cm × 2.5 cm × 2.5 cm) ion cell. Samples were introduced to the system with variable leak valves maintained at ambient temperatures. Typically, a sample pressure of ca. 1×10^{-7} torr, measured with a Granville Phillip Gauge Controller Series 280, was employed for all studies. Electron impact ionization of the sample was performed with 50 eV (nominal) of ionizing energy and 100 ± 10 nA of emission current. The ion cell trapping voltage was typically maintained at 1.25 V (50 V/m).

Ion-ejection techniques were used to mass-select a particular reactant ion. The procedures utilized for these studies have been described previously and are analogous to those used for collision-induced dissociation.[34,35] In all experiments the ion ejection frequencies were selected so as to minimize the translational excitation of the reactant ion. For example, the ion ejection oscillator was swept over a minimum mass range at the maximum allowable sweep rate (typically 50 Hz/μs) to accomplish the ion ejection. To assure that translational energy effects were negligible, the relative reaction rates were obtained by using several ion ejection radio frequency ranges, oscillator amplitudes, and sweep rates to ensure that good reproducibility of reactivities was obtained. For example, when the ion ejection oscillator is swept over a mass beginning 5 amu from the Cr^+ ion, a peak at m/z 188 corresponding to $Cr_2(CO)_3^+$ is present. However, as the ion ejection oscillator is moved to 10 or 15 amu away from the Cr^+ ion, the $Cr_2(CO)_3^+$ peak becomes less intense and eventually disappears. If the ion ejection oscillator is swept from 15 to 25 amu from the Cr^+ ion, there is no significant change in the mass spectrum.

A diagram depicting the experimental sequence is shown in Figure 1. The quench pulse ejects any trapped ions in the cell before formation of new ions. The electron beam ionizes the sample by electron impact. Once the sample is ionized, the ion ejection oscillators are swept over the desired mass range. A variable delay time between ion ejection and ion detection is used to control the ion–molecule reaction time. This delay time is the reaction time used to calculate the relative ion–molecule reaction rates.

Relative ion–molecule reaction rates were calculated by plotting the log (I/I_0) vs. time (where I_0 is the initial intensity of a given ion and I is the intensity of the ion at a particular reaction time). To obtain relative reaction rates for secondary and higher-order reactions, I_0 was defined at the time corresponding to the maximum intensity of the precursor ion. For example, in the study of $Cr_2(CO)_4^+$, the intensity (I_0) of the ion reaches a maximum at approximately 125 ms (at 1×10^{-7} torr of $Cr(CO)_6$). At longer reaction times the intensity (I) of this ion decreases due to reaction with neutral $Cr(CO)_6$. The rate constants obtained in this manner were then normalized to the ion–molecule reaction rate for the $M(CO)_x^+$ ion.

The rates of decay for secondary ions, e.g., $Cr_2(CO)_4^+$, have not been corrected for the abundance of the precursor ion, e.g., Cr^+. The data analysis method reported by Ridge[20] did incorporate such a correction.

(12) Armentrout, P. B. *J. Chem. Phys.* **1982**, *76*, 2449.
(13) Halle, L. F.; Armentrout, P. B.; Beauchamp, J. L. *Organomet. Chem.* **1982**, *1*, 963.
(14) George, P. M.; Beauchamp, J. L. *J. Chem. Phys.* **1982**, *76*, 2959.
(15) Foster, M. S.; Beauchamp, J. L. *J. Am. Chem. Soc.* **1975**, *97*, 4808.
(16) Foster, M. S.; Beauchamp, J. L. *J. Am. Chem. Soc.* **1975**, *97*, 4814.
(17) Corderman, R. R.; Beauchamp, J. L. *Inorg. Chem.* **1976**, *15*, 665.
(18) Allison, J.; Ridge, D. P. *J. Am. Chem. Soc.* **1979**, *101*, 4998.
(19) Weddle, G. H.; Allison, J.; Ridge, D. P. *J. Am. Chem. Soc.* **1977**, *99*, 105.
(20) Wronka, J.; Ridge, D. P. *J. Am. Chem. Soc.* **1984**, *106*, 67.
(21) Burnier, R. C.; Byrd, G. D.; Carlin, T. J.; Wise, M. B.; Cody, R. B.; Freiser, B. S. *Int. J. Mass Spectrom. Ion Phys.* **1980**, *33*, 37.
(22) Burnier, R. C.; Byrd, G. D.; Freiser, B. S. *J. Am. Chem. Soc.* **1981**, *103*, 4360.
(23) Tsarbopoulos, A.; Allison, J. *Organomet. Chem.* **1984**, *3*, 86.
(24) Kappes, M. M.; Staley, R. H. *J. Phys. Chem.* **1982**, *86*, 1332.
(25) Uppal, J. S.; Staley, R. H. *J. Am. Chem. Soc.* **1982**, *104*, 1238.
(26) Corderman, R. R.; Beauchamp, J. L. *Inorg. Chem.* **1978**, *17*, 68.
(27) Armentrout, P. B.; Beauchamp. J. L. *J. Am. Chem. Soc.* **1981**, *103*, 6628.
(28) Ervin, K.; Loh, S. K.; Aristov, N.; Armentrout, P. B. *J. Phys. Chem.* **1983**, *87*, 3593.
(29) Michalopoulos, D. L.; Geusic, M. E.; Hansen, S. G.; Powers, D. E.; Smalley, R. E. *J. Phys. Chem.* **1982**, *86*, 3914.
(30) Powers, D. E.; Hansen, S. G.; Geusic, M. E.; Pulu, A. C.; Hopkins, J. B.; Dietz, T. G.; Duncan, M. A.; Langridge-Smith, P. R. R.; Smalley, R. E. *J. Phys. Chem.* **1982**, *86*, 2556.
(31) Dietz, T. G.; Duncan, M. A.; Powers, D. E.; Smalley, R. E. *J. Chem. Phys.* **1981**, *74*, 6511.
(32) Duncan, M. A.; Powers, D. E.; Smalley, R. E. *Chem. Phys.* **1979**, *44*, 415.
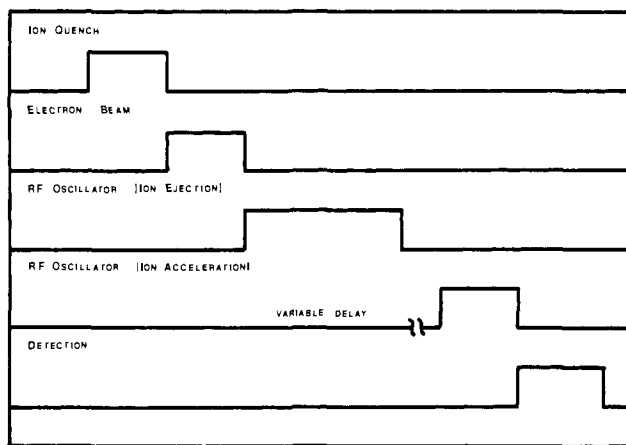(33) Duncan, M. A.; Dietz, T. G.; Smalley, R. E. *J. Am. Chem. Soc.* **1981**, *103*, 5245.

(34) For a discussion of ion cyclotron resonance spectrometry, double resonance, and ion ejection techniques, see: Lehman. T. A.; Bursey, M. N. "Ion Cyclotron Resonance Spectrometry"; Wiley-Interscience: New York, 1976.
(35) Cody, R. B.; Burnier, R. C.; Freiser, B. S. *Anal. Chem.* **1982**, *54*, 961.
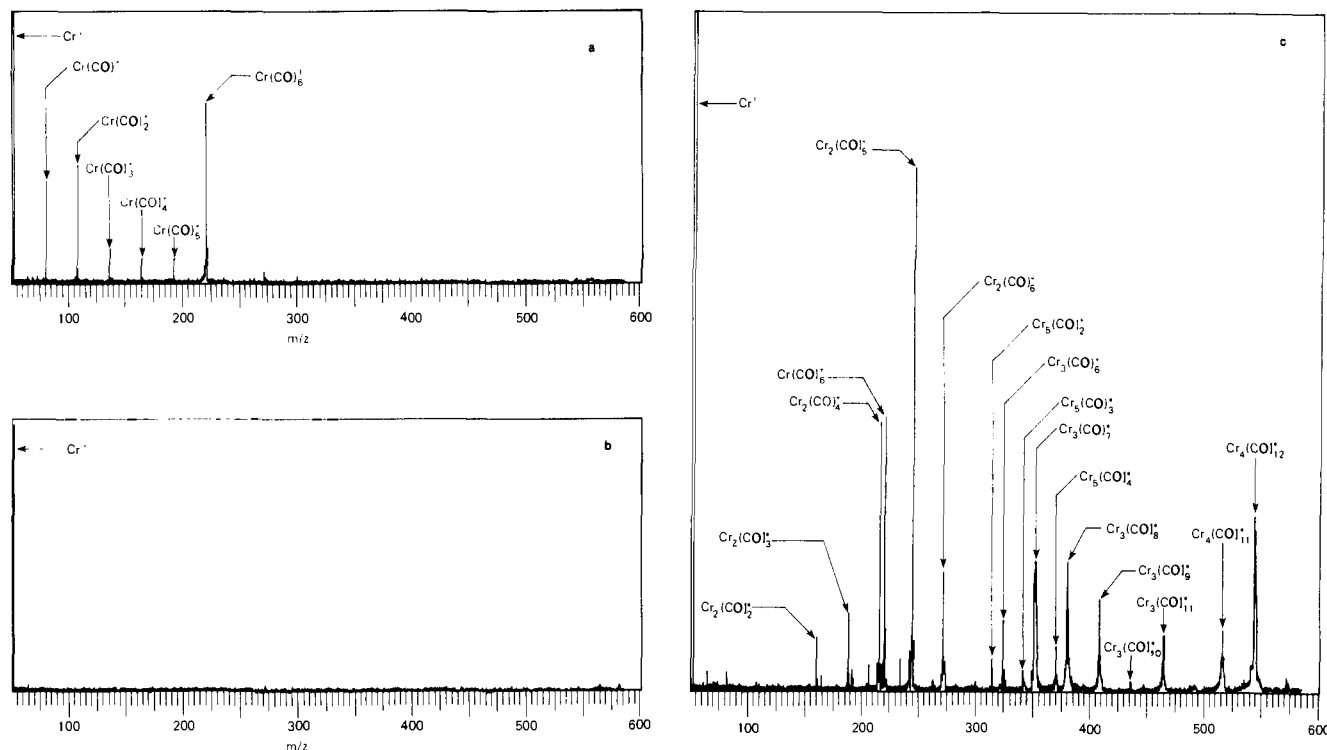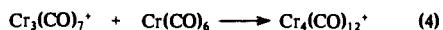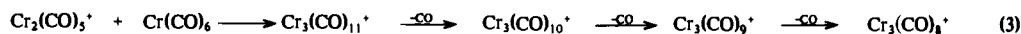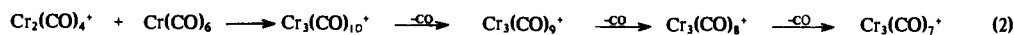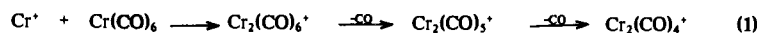
Figure 2. (a) Electron impact mass spectrum of $Cr(CO)_6$. (b) The same spectrum as found in part a except all ions have been ejected by sweeping the external radio frequency oscillator between m/z 62 and 220. (c) The same spectrum as part b except a delay of 500 ms is imposed following ion ejection and ion detection.

Scheme I

However, by comparing the relative reaction rates obtained by the method described above and Ridge's method, we estimate the error introduced by our method to be less than ±10%. The reason we chose not to make such corrections is that for some ions, e.g., $Cr_2(CO)_5^+$, the abundance of the precursor ion (Cr^+) had decayed to zero by the time the product ion, e.g., $Cr_2(CO)_5^+$, had begun to decay. The consequence of our data analysis is that the relative reactivities for highly reactive ions will be underestimated, but the errors of the calculated decay rates are still less than ±10-15%. We feel that the error bars of ±10-15% are within the precision of the measurements. Also, the central issue of this paper deals with ionic cluster fragments which have low ion–molecule reactivities, and relatively small errors for highly reactive species do not effect the final conclusions.

Electron deficiencies were calculated by using the Effective Atomic Number rule; the total number of valence electrons was subtracted from $n \times 18$ and divided by n (n = the number of metal atoms present).[36] In calculating the total number of valence electrons, it is assumed that the structures of the clusters are the triangular polyhedra found in boron hydrides. (See Discussion Section.)

Results

In this report, the ion–molecule reactions of the $Cr(CO)_6$ and $Fe(CO)_5$ systems are examined by using Fourier transform mass spectrometry (FTMS). Electron impact ionization (50 eV nominal energy) of the metal carbonyl, $M(CO)_y$, produces a series of metal-containing ions, viz., $M(CO)_x^+$ ($x = 0-y$). To study the ion–molecule chemistry of a particular ion the initial reactant ion is mass-selected by using ion ejection techniques.[34] A suitable delay time is selected following ion ejection, during which time the ion is allowed to react with the neutral molecule. A typical
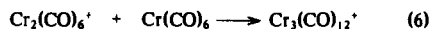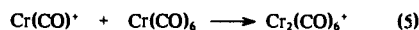
(36) Wade, K. "Transition Metal Clusters"; Johnson, B. F. G., Ed.; John Wiley & Sons: New York, 1980 Chapter 3, p 193.

experimental sequence is contained in Figure 2 for the Cr^+ ion reacting with $Cr(CO)_6$. The normal electron impact ionization (50 eV) mass spectrum of $Cr(CO)_6$ is contained in Figure 2a. The spectrum in Figure 2b was obtained by ejecting all ions between m/z 62 and 220. Figure 2c is the same as Figure 2b except a 500-ms delay was imposed between ion ejection and detection to allow Cr^+ to react with neutral $Cr(CO)_6$. That is, Figure 2c contains all the cluster ions formed in a 500-ms reaction time by the Cr^+ reactant ion.

The major advantage in using the ion ejection technique to select the primary reactant ion is to obtain relative reactivities of the various reactant ions, i.e., M^+ or $M(CO)_x^+$, and to follow a specific sequence of reactions leading to cluster formation. In this study we have not attempted to measure absolute reaction rates. The instrument used for these studies is not equipped with devices for accurately measuring the pressure of the neutral. In the following sections a detailed analysis for the cluster sequences of $Cr(CO)_6$ and $Fe(CO)_5$ systems are presented. Although the general reaction sequences of these systems have many similarities, each system manifests characteristics differences.

$Cr(CO)_6$. Direct ionization of $Cr(CO)_6$ produces intense ions corresponding to $Cr(CO)_x^+$ ($x = 0, 1, 2, 6$). The relative abundances for the $Cr(CO)_3^+$, $Cr(CO)_4^+$, and $Cr(CO)_5^+$ ions are much less (<10%), and these ions have not been investigated thoroughly; however, $Cr(CO)_3^+$, $Cr(CO)_4^+$, and $Cr(CO)_5^+$ give rise to the same cluster ions (in terms of elemental composition) as does $Cr(CO)_2^+$. The largest cluster fragment produced by the reaction of Cr^+ with $Cr(CO)_6$ is $Cr_4(CO)_{12}^+$. The $Cr_4(CO)_{12}^+$ ion is formed by sequential reactions involving $Cr_2(CO)_x^+$ ($x = 4-6$) and $Cr_3(CO)_x^+$ ($x = 7-12$). A general reaction sequence is summarized in Scheme I. (Only the major (>20%) ionic cluster

Scheme II

$$Cr(CO)^+ + Cr(CO)_6 \longrightarrow Cr_2(CO)_6^+ \quad (5)$$

$$Cr_2(CO)_6^+ + Cr(CO)_6 \longrightarrow Cr_3(CO)_{12}^+ \quad (6)$$

Scheme III

$$Cr(CO)_2^+ + Cr(CO)_6 \longrightarrow Cr_2(CO)_7^+ \xrightarrow{-CO} Cr_2(CO)_6^+ \quad (7)$$

$$Cr_2(CO)_7^+ + Cr(CO)_6 \longrightarrow Cr_3(CO)_{12}^+ \quad (8)$$

fragments are included in the reaction schemes.) The general reaction schemes were confirmed by using ion ejection techniques and by following the temporal distribution of the product ions. The Cr^+ ion reacts with neutral $Cr(CO)_6$ to produce three dinuclear species of $Cr_2(CO)_x^+$ ($x = 4-6$). These three dinuclear cluster fragments react with $Cr(CO)_6$ to form $Cr_3(CO)_x^+$ ($x = 7-12$) (reaction 2 and 3). The trinuclear cluster fragments react to produce $Cr_4(CO)_{12}^+$ (reaction 4). A temporal distribution of the various cluster fragments initiated by the Cr^+ ion is shown in Figure 3. The data in Figure 3 give the relative abundance for each of the ionic cluster fragments, e.g., percent total ion current versus time.

The clustering sequence for the $Cr(CO)_+$ ion differs markedly from that for Cr^+. For example, $Cr(CO)^+$ reacts with $Cr(CO)_6$ to form $Cr_2(CO_6)^+$ (reaction 5). This ionic cluster fragment is 0.05 times less reactive than the $Cr(CO)^+$ ion, but it does react very slowly with $Cr(CO)_6$ to produce $Cr_3(CO)_{12}^+$ (m/z 492). In sharp contrast to $Cr_3(CO)_7^+$ and $Cr_3(CO)_8^+$ formed by reaction of Cr^+, the $Cr_3(CO)_{12}^+$ ion produced by reaction 6 does not react further with $Cr(CO)_6$ to produce additional cluster fragments (Scheme II). $Cr(CO)_2^+$, gives rise to both $Cr_2(CO)_6^+$ and $Cr_2(CO)_7^+$ (reaction 7). Again the $Cr_2(CO)_6^+$ ion is slow to react with $Cr(CO)_6$, whereas $Cr_2(CO)_7^+$ reacts with $Cr(CO)_6$ to produce an intense ion corresponding to $Cr_3(CO)_{12}^+$. It is interesting to note that the $Cr(CO)^+$ and $Cr(CO)_2^+$ reaction sequences terminate at $Cr_3(CO)_{12}^+$, whereas the Cr^+ initiated cluster sequence terminates at $Cr_4(CO)_{12}^+$. An overall reaction sequence for $Cr(CO)_2^+$ is contained in Scheme III (reactions 7 and 8).

The ion-molecule reactions of the $Cr(CO)_6$ system illustrate the influence that the nature of the initial reactant ion has on the clustering process. That is, in general, the M^+ and $M(CO)_x^+$ ions react to give different ionic cluster fragments, and the reaction rates of the M^+ and $M(CO)_x^+$ ions differ significantly. This control over the clustering process could prove important as a means of investigating the chemical reactivity of specific cluster ions. These aspects of the clustering process are discussed further in a later section.

$Fe(CO)_5$. Direct ionization of $Fe(CO)_5$ produces intense ions corresponding to $Fe(CO)_x^+$, $x = 0-4$. The reactions of $Fe(CO)_2^+$ and $Fe(CO)_3^+$ with neutral $Fe(CO)_5$ were not investigated thoroughly because neither ion can be mass selected with ion ejection methods without affecting the ion's translational energy. The ion cyclotron frequency (ω) has an m^{-1} dependence on mass, e.g., $\omega = eB/m$.[37] Consequently, the frequency difference for two ions separated by 28 amu gets smaller as the mass of the ion increases. When the ion ejection oscillator is swept over a frequency range beginning 15 amu from the Fe^+ ion, $Fe(CO)^+$ is readily ejected, and there is no indication that Fe^+ receives any translational excitation. On the other hand, if the radio frequency oscillator is swept over a frequency range starting 15 amu away from $Fe(CO)_2^+$, the resulting spectrum contains both $Fe(CO)_2^+$ and $Fe(CO)_3^+$. If the radio frequency amplitude is increased to a level sufficient to eject $Fe(CO)_3^+$, it is rather obvious that $Fe(CO)_2^+$ has been sufficiently excited (translationally) to alter the ion-molecule product. Rather than go to great lengths to minimize these effects, the results of which would be questionable, we have elected not to study the detailed reactivities of $Fe(CO)_2^+$ and $Fe(CO)_3^+$. However, the details of translational energy effects on the ion-molecule chemistry of these fragments will be described
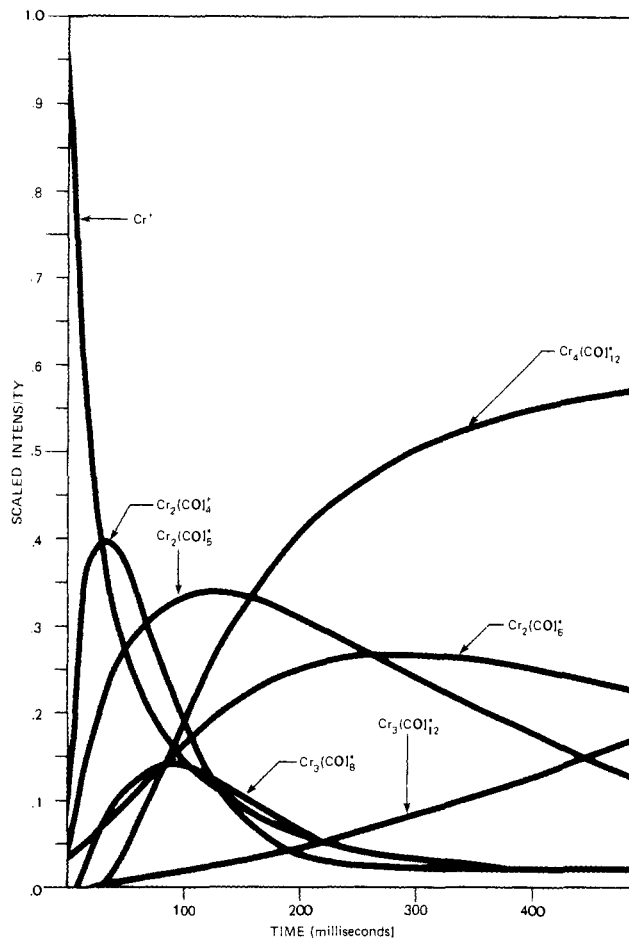
(37) Comisarow, M. B.; Marshall, A. G. *J. Chem. Phys.* **1976**, *64*, 110.

Figure 3. Temporal distribution of cluster fragments formed when Cr^+ reacts with $Cr(CO)_6$.

in a separate paper. It should be noted that due to the small intensity of $Cr(CO)_3^+$, we are able to mass-select the $Cr(CO)_2^+$ ion without translational energy effects.
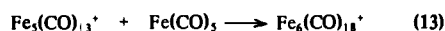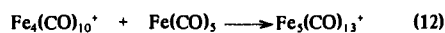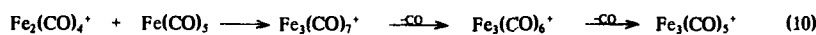
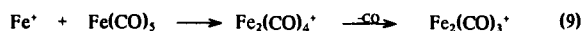The largest cluster fragment produced by the reaction of Fe^+ with $Fe(CO)_5$ is $Fe_6(CO)_{18}^+$. The $Fe_6(CO)_{18}^+$ ion is formed by sequential reactions of $Fe_2(CO)_x^+$, $Fe_3(CO)_x^+$, $Fe_4(CO)_x^+$, and $Fe_5(CO)_x^+$. A general reaction sequence is summarized in Scheme IV. Fe^+ reacts with neutral $Fe(CO)_5$ to produce $Fe_2(CO)_3^+$ and $Fe_2(CO)_4^+$ (reaction 9). These cluster fragments react to produce $Fe_3(CO)_x^+$ ($x = 5-7$) (reaction 10). The trinuclear cluster fragments react to form $Fe_4(CO)_x^+$ ($x = 8-10$ and 12) (reaction 11). This clustering sequence continues with $Fe_4(CO)_x^+$ producing $Fe_5(CO)_{13}^+$ (reaction 12) which gives rise to $Fe_6(CO)_{18}^+$ (reaction 13).

The reaction sequences for $Fe(CO)^+$ and $Fe(CO)_4^+$ are summarized in Schemes V and VI, respectively. Note that Scheme V terminates with $Fe_5(CO)_{13}^+$, and Scheme VI terminates with $Fe_4(CO)_9^+$, whereas Scheme IV terminates with $Fe_6(CO)_{18}^+$. Also, each scheme in the $Fe(CO)_5$ system is associated with its own unique ions. For example, $Fe(CO)^+$ produces both $Fe_2(CO)_5^+$ and $Fe_4(CO)_{11}^+$. These ions are not formed by reaction of Fe^+ (Scheme IV). The $Fe_2(CO)_6^+$, $Fe_2(CO)_7^+$, and $Fe_3(CO)_{10}^+$ ions are formed only by the $Fe(CO)_4^+$ reactant ion (Scheme VI).

Discussion

Closer examination of Schemes I-VI reveals that while the ion-molecule reaction sequences for the $Cr(CO)_6$ and $Fe(CO)_5$ systems appear to be similar, each has its characteristic differences. For example, the largest cluster fragment produced in the $Cr(CO)_6$ system is $Cr_4(CO)_{12}^+$ while the largest cluster fragment formed in the $Fe(CO)_5$ system is $Fe_6(CO)_{18}^+$. Comparison of Scheme II (initial reactant ion being $Cr(CO)^+$) and Scheme V ($Fe(CO)^+$ the reactant ion) also illustrates the similarities and differences found in the two systems. For instance, the addition of a CO

Scheme IV

$$Fe^+ + Fe(CO)_5 \longrightarrow Fe_2(CO)_4^+ \xrightarrow{-CO} Fe_2(CO)_3^+ \quad (9)$$

$$Fe_2(CO)_4^+ + Fe(CO)_5 \longrightarrow Fe_3(CO)_7^+ \xrightarrow{-CO} Fe_3(CO)_6^+ \xrightarrow{-CO} Fe_3(CO)_5^+ \quad (10)$$

$$Fe_3(CO)_7^+ + Fe(CO)_5 \longrightarrow Fe_4(CO)_{12}^+ \xrightarrow{-2CO} Fe_4(CO)_{10}^+ \xrightarrow{-CO} Fe_4(CO)_9^+ \xrightarrow{-CO} Fe_4(CO)_8^+ \quad (11)$$

$$Fe_4(CO)_{10}^+ + Fe(CO)_5 \longrightarrow Fe_5(CO)_{13}^+ \quad (12)$$

$$Fe_5(CO)_{13}^+ + Fe(CO)_5 \longrightarrow Fe_6(CO)_{18}^+ \quad (13)$$

Scheme V

$$Fe(CO)^+ + Fe(CO)_5 \longrightarrow Fe_2(CO)_5^+ \xrightarrow{-CO} Fe_2(CO)_4^+ \quad (14)$$

$$Fe_2(CO)_4^+ + Fe(CO)_5 \longrightarrow Fe_3(CO)_8^+ \xrightarrow{-CO} Fe_3(CO)_7^+ \quad (15)$$

$$Fe_3(CO)_7^+ + Fe(CO)_5 \longrightarrow Fe_4(CO)_{12}^+ \xrightarrow{-CO} Fe_4(CO)_{11}^+ \quad (16)$$

$$Fe_4(CO)_{11}^+ + Fe(CO)_5 \longrightarrow Fe_5(CO)_{13}^+ \quad (17)$$

Scheme VI

$$Fe(CO)_4^+ + Fe(CO)_5 \longrightarrow Fe_2(CO)_7^+ \xrightarrow{-CO} Fe_2(CO)_6^+ \quad (18)$$

$$Fe_2(CO)_6^+ + Fe(CO)_5 \longrightarrow Fe_3(CO)_{10}^+ \xrightarrow{-4CO} Fe_3(CO)_6^+ \quad (19)$$

$$Fe_3(CO)_{10}^+ + Fe(CO)_5 \longrightarrow Fe_4(CO)_{12}^+ \xrightarrow{-3CO} Fe_4(CO)_9^+ \quad (20)$$

ligand to the bare metal ion has the same effect on both systems. The Cr^+ reaction scheme (Scheme I) and the Fe^+ reaction scheme (Scheme IV) terminate with $Cr_4(CO)_{12}^+$ and $Fe_6(CO)_{18}^+$, respectively. However, when the intial reactant ion is either $Cr(CO)^+$ or $Fe(CO)^+$, the reaction scheme (Schemes II and V) terminates with a cluster fragment which contains one less metal atom, e.g., $Cr_3(CO)_{12}^+$, $Fe_5(CO)_{13}^+$. A notable difference between these two reaction schemes is the ions formed by the reaction of $Cr(CO)^+$ with $Cr(CO)_6$ are also formed by reaction of Cr^+ with $Cr(CO)_6$. Conversely, $Fe(CO)^+$ gives abundant $Fe_2(CO)_5^+$ and $Fe_4(CO)_{11}^+$ ions, which are not formed by reaction of Fe^+ with $Fe(CO)_5$.

We are proposing that the differences in the ion–molecule reaction chemistry of these systems can be understood by examining the electron deficiencies of the cluster fragments, as well as considering the effects of excess internal energy. Various methods for electron counting in metal carbonyl clusters have been proposed.[38,39] These electron counting methods give two limiting cases for the number of valence electrons per atom: low nuclearity clusters (18 valence electrons) and standard infinite metallic lattices (12 valence electrons). The bonding in low nuclearity clusters gives rise to simple triangular polyhedra structures, whereas the large nuclearity clusters have cubic closed-packed (infinite metallic lattice) structures.[40] We have chosen to use the 18-electron model because of the low nuclearity of the ionic cluster fragments. Similar models have been proposed by Ridge et al.[20]

The electron deficiency (ED) of a particular ionic cluster fragment can be calculated by using the 18-electron rule (eq I)[36]

$$ED = 18 \times n - (\text{total no. of valence electrons in the cluster})/n \quad (I)$$

where n equals the number of metal atoms in the cluster fragment. When calculating electron deficiencies, it is assumed that the cluster fragments have the structures found in the triangular polyhedra of the boron hydrides. For example, to calculate the electron deficiency of $Fe_4(CO)_{12}^+$, we have assumed that this cluster fragment is a tetrahedron; therefore, each metal is bonded to three metal atoms, and the number of valence electrons on each metal is 11 (8 electrons in the valence orbitals of Fe plus 3
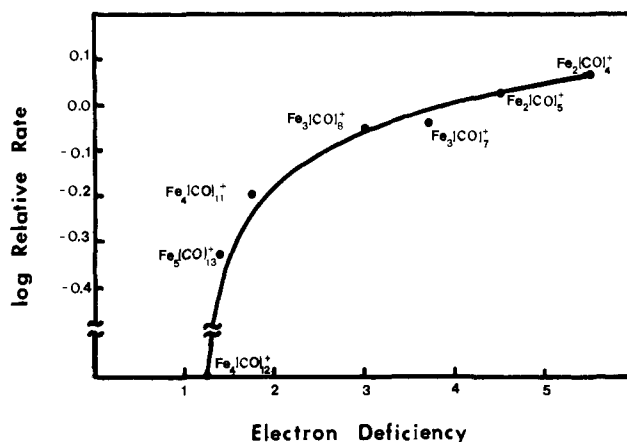

Figure 4. Plot of log relative rate vs. calculated electron deficiencies for $Fe(CO)^+/Fe(CO)_5$. Calculated electron deficiencies are based on simple polyhedra models of boron hydrides.

metal–metal bonds). The CO ligands are considered to be 2-electron donors. Thus, by this method we obtain an electron deficiency of 1.25 for $Fe_4(CO)_{12}^+$ (eq II). If the positive charge

$$ED_{Fe_4(CO)_{12}^+} = 18 \times 4 - [(4 \times 11) + (12 \times 2) - 1]/4 = 1.25 \quad (II)$$

on the cluster fragment had not been considered, the electron deficiency for $Fe_4(CO)_{12}^+$ would be 1.0. Therefore, this electron deficiency of 1.25 indicates that there is an open coordination site on each Fe atom for a 1-electron donor. (This seems to be a good assumption since the charge on the cluster fragment will be delocalized over the cluster).

Since the electron deficiency is an indication of the number of open coordination sites on a metal atom, then it follows that as the electron deficiency of the cluster fragments increases, the relative reaction rates should also increase.[20] For example, a cluster fragment with a high electron deficiency will have several open coordination sites on each metal atom, which will increase the rate for ion–molecule reactions. On the basis of this concept, $Fe_2(CO)_4^+$, which has an electron deficiency of 5.5, should have a larger relative reaction rate than $Fe_4(CO)_{12}^+$ (electron deficiency of 1.25). An additional consequence of this concept is that the small ionic cluster fragments, e.g., $Cr_2(CO)_4^+$, $Fe_2(CO)_4^+$, etc., should be more reactive than the larger, more coordinatively saturated clusters, e.g., $Cr_4(CO)_{12}^+$, $Fe_6(CO)_{18}^+$, etc. On the basis of this relatively simple concept, a plot of the log relative reaction rate vs. electron deficiency should increase in a monotonic manner.[20] In general, this trend is observed; however, there are notable exceptions when this trend is not followed. Such data for the $Fe(CO)^+/Fe(CO)_5$ system are contained in Figure 4. For this system, the electron deficiencies of the ionic cluster fragments were calculated by assuming single metal–metal bonds and CO acting as a 2-electron donor. The correlation between reactivity and electron deficiency for the $Fe(CO)^+/Fe(CO)_5$ system is excellent.

Figure 5 shows the reactivity vs. electron deficiency data for the $Fe^+/Fe(CO)_5$ system. It is rather obvious that the simple relationship between electron deficiency and reactivity breaks down for this system. Up to this point we have only considered single metal–metal bonds and CO acting as a 2-electron donor in obtaining the electron deficiencies. However, it is well-known that CO is capable of acting as a 4- or 6-electron donor and that transition metals are capable of multiple metal–metal bonding. For example, the butterfly metal cluster $[Me_3NCH_2Ph][Fe_4(CO)_{13}H]$ is known to contain 12 terminally bonded CO's, with

(38) Lauher, Joseph W. *J. Am. Chem. Soc.* **1978**, *100*, 5305.
(39) Wade, K. *Adv. Inorg. Radiochem.* **1976**, *18*, 1.
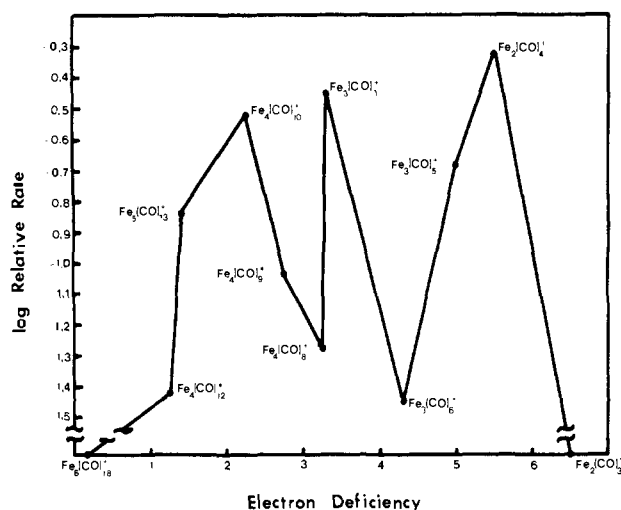(40) Chini, P. *J. Organomet. Chem.* **1980**, *200*, 37.

Formation of Transition-Metal Carbonyl Cluster Fragments

J. Am. Chem. Soc., Vol. 107, No. 13, 1985 3767

Figure 5. Plot of log relative rate vs. calculated electron deficiencies for the $Fe^+/Fe(CO)_5$ system. Calculated electron deficiencies are based on simple polyhedra models of boron hydrides.

Electron Deficiency

Figure 6. Plot of log relative rate vs. electron deficiency for the $Fe^+/Fe(CO)_5$ system. In this system, the electron deficiencies were calculated by assuming that some of the cluster fragments contain multiple metal-metal bonds and/or carbonyl ligands acting as 4-electron donors.

the remaining CO being "trapped among the two butterfly wings in an unusual bonding situation".[41] This CO acts as a 4-electron donor, allowing the metal cluster to achieve its noble gas (18 electron) configuration. Another example of 4-electron donor CO ligand is found in the reaction of CO with alkyl and hydride derivatives of bis(pentamethylcyclopentadienyl)zirconium.[42-44] Once again, this ligand enables the zirconium atom to achieve a full 18-electron configuration. Wade has pointed out that this type of bonding may not be uncommon among coordinatively unsaturated reaction intermediates.[36] Owing to the nature of the ionic cluster fragments formed by ion-molecule reactions, it is reasonable to suspect that these ions may also show unusual bonding of the ligands and possibly the metal centers.

The subject of multiple bonds among metal atoms is well researched.[15] However, because the metal d electrons needed for the π and δ bonds in metal-metal bonding can be drawn into the π^* orbitals of the ligand, strong π acid ligands, such as CO, usually prohibit the presence of multiple metal-metal bonds.[40] Even in these systems, however, evidence for multiple metal bonds has been proposed. The proposed multiple metal bonding found in transition metal cluster fragments is for anionic species, e.g., $Cr_2(CO)_8^-$ is believed to contain a triple metal-metal bond, and $Cr_2(CO)_6^-$ has an even higher bond order.[46] Also, Ridge has suggested the existence of multiple metal-metal bonds in the $Fe_x(CO)_y^-$ (x=2; y=5-7) ionic cluster fragments.[20]

In considering the ionic cluster fragments formed in the ion-molecule reaction of Fe^+ with $Fe(CO)_5$, it is important to consider the coordination unsaturation of these ions. For instance $Fe_2(CO)_3^+$ and $Fe_2(CO)_4^+$ appear to have electron deficiencies of 6.5 and 5.5, respectively. $Fe_2(CO)_4^+$ compensates for this high electron deficiency by reacting with the neutral $Fe(CO)_5$. $Fe_2(CO)_3^+$, on the other hand, has no measureable reactivity. It is reasonable that $Fe_2(CO)_3^+$ compensates for its high electron deficiency by forming triple metal-metal bonds and the CO acting as a 4-electron donor. This hypothesis can be rationalized by considering that the iron atoms (due to their electron deficiency) localize the metal d electrons rather than use them for ligand binding. Figure 6 contains the reactivity vs. electron deficiency data for the $Fe^+/Fe(CO)_5$ system. This graph was obtained by
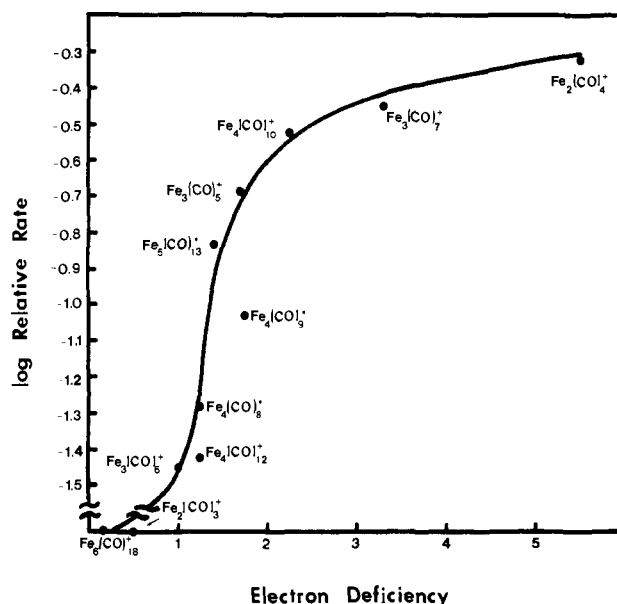
altering the electron deficiencies of ionic cluster fragments showing the greatest deviation in Figure 5, e.g., $Fe_2(CO)_3^+$, $Fe_3(CO)_5^+$, $Fe_3(CO)_6^+$, $Fe_4(CO)_8^+$, and $Fe_4(CO)_9^+$. The relative reactivies for these ionic cluster fragments suggest that the electron deficiencies are significantly smaller than expected on the basis of the simple polyhedra model. Thus, it is apparent that the metal centers of these ionic cluster fragments are relatively strong Lewis acids. On the other hand, for those ionic cluster fragments which show a good correlation between the reactivity and electron deficiency, the metal center acts as a Lewis base. Structures such as I and II were used to calculate the electron deficiencies which are consistent with the observed reactivity. It should be noted that a 4-electron donating CO decreases the electron deficiency by the same amount as does a double metal-metal bond. (Exact determination of these structures cannot be delineated by the present experimental technique.) These model structures are derived by assuming that each metal atom tends toward a noble gas configuration (or as close to one as possible) and that the electron density in the cluster should be delocalized throughout that cluster.

I

II
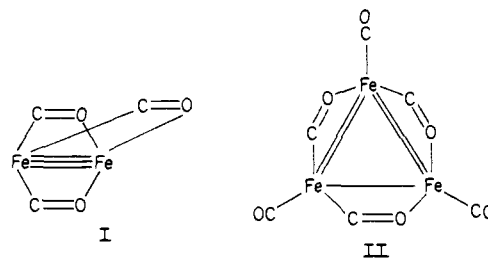
The fragment ions for each reaction sequence were treated in a similar manner. The relative reactivities for ionic cluster fragments which did not correlate with the calculated electron deficiency were assumed to have multiple metal-metal bonds and/or carbonyl ligands acting as 4-electron donors. Tables I and II list the ionic cluster fragments formed by the various reactant ions for the $Cr(CO)_6$ and $Fe(CO)_5$ systems, as well as the relative reaction rate and electron deficiency of each of the fragment ions. (The positive charge on the ionic cluster fragments was considered to be a part of the valence electrons and was included in the calculation of the electron deficiencies.) The column marked ED* indicates the electron deficiency obtained by assuming multiple metal-metal bonds and/or CO acting as a 4-electron donor. In the $Cr(CO)^+/Cr(CO)_6$ system, there are not sufficient data points

(41) Manassero, M.; Sansoni, M.; Longoni, G. *J. Chem. Soc., Chem. Commun.* **1976**, *919*.

(42) Manriquez, J. M.; McAlister, D. R.; Sanner, R. D.; Bercaw, J. E. *J. Am. Chem. Soc.* **1978**, *100*, 2716.

(43) Berry, D. H.; Bercaw, J. E.; *J. Am. Chem. Soc.* **1982**, *104*, 4712.

(44) Threlkel, R. S.; Bercaw, J. E. *J. Am. Chem. Soc.* **1981**, *103*, 2650.

(45) Cotton, F. A.; Walton, R. A. "Multiple Bonds Between Metal Atoms"; John Wiley & Sons: New York, 1982, p 1.

(46) Dunbar, R. C.; Ennever, J. L.; Fackler, J. P., Jr. *Inorg. Chem.* **1973**, *12*, 2734.

Table I. Ionic Cluster Fragments of the $Cr(CO)_6$ System

ion	log rel rate[a]	electron deficiency	ED*[b]
reactant ion = Cr^+			
$Cr_2(CO)_4^+$	+0.164	7.5	
$Cr_2(CO)_5^+$	−0.407	6.5	4.5
$Cr_2(CO)_6^+$	−0.665	5.5	3.5
$Cr_3(CO)_7^+$	−0.028	5.67	
$Cr_3(CO)_8^+$	−0.128	5.0	
$Cr_3(CO)_{11}^+$	$-\infty$[c]	3.0	
$Cr_4(CO)_{12}^+$	$-\infty$	3.25	
reactant ion = $Cr(CO)^+$			
$Cr_2(CO)_6^+$	−1.31	5.5	
$Cr_3(CO)_{12}^+$	$-\infty$	2.3	
reactant ion = $Cr(CO)_2^+$			
$Cr_2(CO)_6^+$	−0.860	5.5	2.5
$Cr_2(CO)_7^+$	−0.818	4.5	
$Cr_3(CO)_{12}^+$	$-\infty$	2.3	

[a] The rate of the ionic cluster fragments is relative to the rate of the reactant ion. [b] The column marked ED* refers to the electron deficiency calculated by assuming multiple metal–metal bonds and/or 4-electron donor carbonyl ligands are present. [c] The log relative rate is defined as $-\infty$ for those cluster fragments which have no discernible rate.

Table II. Ionic Cluster Fragments of the $Fe(CO)_5$ System

ion	log rel rate[a]	electron deficiency	ED*[b]
reactant ion = Fe^+			
$Fe_2(CO)_3^+$	$-\infty$[c]	6.5	0.5
$Fe_2(CO)_4^+$	−0.326	5.5	
$Fe_3(CO)_5^+$	−0.682	5.0	1.67
$Fe_3(CO)_6^+$	−1.45	4.3	1.0
$Fe_3(CO)_7^+$	−0.453	3.67	
$Fe_4(CO)_8^+$	−1.28	3.25	1.25
$Fe_4(CO)_9^+$	−1.03	2.75	1.75
$Fe_4(CO)_{10}^+$	−0.520	2.25	
$Fe_4(CO)_{12}^+$	−1.42	1.25	
$Fe_5(CO)_{13}^+$	−0.833	1.4	
$Fe_6(CO)_{18}^+$	$-\infty$	0.167	
reactant ion = $Fe(CO)^+$			
$Fe_2(CO)_4^+$	+0.124	5.5	
$Fe_2(CO)_5^+$	+0.057	4.5	
$Fe_3(CO)_7^+$	−0.079	3.67	
$Fe_3(CO)_8^+$	−0.094	3.0	
$Fe_4(CO)_{11}^+$	−0.380	1.75	
$Fe_4(CO)_{12}^+$	$-\infty$	1.25	
$Fe_5(CO)_{13}^+$	−0.654	1.4	
reactant ion = $Fe(CO)_4^+$			
$Fe_2(CO)_6^+$	−0.130	3.5	
$Fe_2(CO)_7^+$	−0.255	1.5	
$Fe_3(CO)_6^+$	$-\infty$	4.3	1.0
$Fe_3(CO)_{10}^+$	$-\infty$	1.67	
$Fe_4(CO)_9^+$	$-\infty$	2.75	1.75
$Fe_4(CO)_{12}^+$	−1.43	1.25	

[a] The rate of the ionic cluster fragments is relative to the rate of the reactant ion. [b] The column marked ED* refers to the electron deficiency calculated by assuming multiple metal–metal bonds and/or 4-electron donor carbonyl ligands are present. [c] The log relative rate is defined as $-\infty$ for those cluster fragments which have no discernible rate.

to produce a meaningful graph. However, it is rather obvious that the reactivity of the $Cr_2(CO)_6^+$ ion is much lower than the electron deficiency of 5.5 would indicate. Therefore, it is highly probable that this ion, like the $Cr_2(CO)_6^+$ formed by Cr^+ and $Cr(CO)_2^+$, has an electron deficiency of less than 5.5, e.g., 2.5–3.5.

By analyzing the data in terms of reaction rate and electron deficiency, it can be determined that some cluster fragments which have the same elemental composition are different in terms of their structure. For example, the $Cr_2(CO)_6^+$ fragment ion can be produced from the Cr^+, $Cr(CO)^+$, and $Cr(CO)_2^+$ ion. When plotting the log relative rate vs. electron deficiency for the

$Cr^+/Cr(CO)_6$ system, the $Cr_2(CO)_6^+$ fragment appears to have an electron deficiency of 3.5. This electron deficiency is consistent with a Cr–Cr triple bond. On the other hand, the $Cr_2(CO)_6^+$ ion formed by reaction of $Cr(CO)_2^+$ appears to have an electron deficiency of 2.5 (suggesting a Cr–Cr quadruple bond).

A basic premise of the above discussion is that ionic cluster fragments with low electron deficiencies are intrinsically more stable than cluster fragments with high electron deficiencies. However, Tables I and II show that some cluster fragments with low electron deficiencies and reactivities lose a ligand(s) to produce other ionic cluster fragments with higher electron deficiencies (presumably less stable). Undoubtedly, the driving force for these reactions is excess internal energy. For example, the $Fe_4(CO)_{12}^+$ ion formed by reaction of Fe^+ with $Fe(CO)_5$ has an electron deficiency of 1.25. The $Fe_4(CO)_{12}^+$ ion expels two CO's to give $Fe_4(CO)_{10}^+$ which has an electron deficiency of 2.25. Owing to the exothermicity of the ion–molecule reaction, the $Fe_4(CO)_{12}^+$ ion is probably formed with excess internal energy and without collisional stabilization decays by unimolecular expulsion of the CO ligands. Loss of these ligands results in a cluster that has a higher electron deficiency (2.25), and is therefore more reactive. Thus, while the reactivity of an ionic cluster fragment is dependent on the electron deficiency, the ionic cluster fragments formed by a given system, e.g., $M(CO)_x^+/M(CO)_y^+$, will depend on the relative stability of the cluster fragment and the energetics of the ion–molecule reaction.

Conclusion

The present work illustrates the range of studies that can be performed with FTMS. A particularly valuable feature of this method is the ability to perform ion ejection to mass-select a specific reactant ion and study its chemistry without competition from other reactant ions. Caution should be used in order to avoid effects from translational excitation of the reactants ions. The present study has been limited to the $Cr(CO)_6$ and $Fe(CO)_5$ system. Although the reaction sequences leading to formation of ionic cluster fragments are associated with many similarities, each system manifests characteristic differences. In particular, these systems show the same general trends for cluster ion formation; however, the ionic cluster fragments vary markedly in the degree of coordination unsaturation and relative reactivities.

Some of the ionic cluster fragments produced by ion–molecule reactions in the $Cr(CO)_6$ and $Fe(CO)_5$ systems contain multiple metal–metal bonds and/or carbonyl ligands that serve as 4-electron donors. This assumption is based on the relationship between the electron deficiencies (calculated from the 18-electron rule) and the relative reactivities of the ionic cluster fragments. An increase in the electron deficiency corresponds to an increase in the reactivity.

The results of our studies suggest that a high degree of chemoselectivity will be observed for the reactions of particular clusters. In particular, we are interested in the reactivities of specific ionic cluster fragments with simple saturated and unsaturated hydrocarbons and the influence that the bond order of the ionic cluster exerts on the reactivity. Specific examples of the studies are reactions leading to C–C and C–H bond insertion; similar reactions of bare metal ions have been extensively studied by several workers.[4-14]